Carcinogenesis, 2018, Vol. 39, No. 10, 1222–1234

doi:10.1093/carcin/bgy097
Advance Access publication July 23, 2018
Original Article

ORIGINAL ARTICLE

Proteomic analysis of the OGT interactome: novel links to epithelial–mesenchymal transition and metastasis of cervical cancer

Jie Gao[1], Yang Yang[1], Rongfang Qiu[1], Kai Zhang[1], Xu Teng[2], Ruiqiong Liu[3] and Yan Wang[1,2,*]

[1]2011 Collaborative Innovation Center of Tianjin for Medical Epigenetics, Tianjin Key Laboratory of Cellular and Molecular Immunology, Key Laboratory of Immune Microenvironment and Disease (Ministry of Education), Department of Biochemistry and Molecular Biology, School of Basic Medical Sciences, Tianjin Medical University, Tianjin 300070, China, [2]Department of Biochemistry and Molecular Biology, School of Basic Medical Sciences, Capital Medical University, Beijing 100069, China and [3]Cancer Center, The Second Hospital of Shandong University, Jinan 250033, China

*To whom correspondence should be addressed. Tel: +86 22 83336946; Fax: +86 22 83336946; Email: yanwang@tmu.edu.cn
Correspondence may also be addressed to Ruiqiong Liu. Tel: +86 0531 85875541; Fax: +86 0531 85875541; Email: l_qiong@outlook.com

Abstract

The role of *O*-GlcNAc transferase (OGT) in gene regulation and tumor invasion is poorly understood. Here, we have identified several previously undiscovered OGT-interacting proteins, including the PRMT5/WDR77 complex, the PRC2 complex, the ten-eleven translocation (TET) family, the CRL4B complex and the nucleosome remodeling and deacetylase (NuRD) complex. Genome-wide analysis of target genes responsive to OGT resulted in identification of a cohort of genes including *SNAI1* and *ING4* that are critically involved in cell epithelial–mesenchymal transition and invasion/metastasis. We have demonstrated that OGT promotes carcinogenesis and metastasis of cervical cancer cells. OGT's expression is significantly upregulated in cervical cancer, and low OGT level is correlated with improved prognosis. Our study has thus revealed a mechanistic link between OGT and tumor progression, providing potential prognostic indicators and targets for cancer therapy.

Introduction

Post-translational modification (PTM) of proteins refers to the covalent addition of chemical modifications after protein biosynthesis. The PTM of proteins increases proteomic diversity and complexity which plays a vital part in almost every normal cell biology as well as during pathogenic processes. Notable among these PTMs is *O*-GlcNAcylation, a newly discovered modification that catalyzes the addition of the single *O*-linked *N*-acetylglucosamine (*O*-GlcNAc) group to Ser and Thr residues of different proteins (1). As a product of the hexosamine biosynthetic pathway, uridine diphosphate GlcNAc is the donor substrate for *O*-GlcNAcylation, which integrates glucose, amino acid, fatty acid and nucleotide metabolism (2). In addition, *O*-GlcNAcylation is considered to be a nutrient and stress sensor that regulates cellular processes including transcription, translation, signal transduction and metabolism (3). Furthermore, disruption of *O*-GlcNAc homeostasis is related to the pathogenesis of many diseases such as cancer, diabetes and neurodegeneration (4–9).

Dynamic changes of *O*-GlcNAcylation are controlled by a unique pair of enzymes: *O*-GlcNAc transferase (OGT), which catalyzes the transfer of GlcNAc and *O*-GlcNAcase, which hydrolyzes the residue (10). Mammalian OGT gene resides on the X chromosome at Xq13.1 in close proximity to the X-inactive specific transcript (XIST) locus and the X-inactivation center, and deletion of OGT leads to lethality of XY stem cells (11,12). The crystalline structure of human OGT has recently been reported (13,14), which is highly conserved in bacteria, higher plants and humans (2,15). Because of alternative splicing, three different isoforms of OGT are generated: nucleocytoplasmic OGT, mitochondrial OGT

Received: February 26, 2018; Revised: June 21, 2018; Accepted: July 22, 2018

Abbreviations

ChIP	chromatin immunoprecipitation
EMT	epithelial–mesenchymal transition
GO	gene ontology
GST	glutathione S-transferase
IB	immunoblotting
ING	inhibitor of growth
IP	immunoprecipitation
mOGT	mitochondrial OGT
NuRD	nucleosome remodeling and deacetylase
O-GlcNAc	O-linked N-acetylglucosamine
OGT	O-GlcNAc transferase
PBS	phosphate-buffered saline
PPI	protein–protein interaction
PTM	post-translational modification
shRNAs	short hairpin RNAs

(mOGT) and short OGT. These three isoforms share common carboxy-terminal catalytic and phosphoinositide-binding domains but differ in the length of their amino-terminal tetratricopeptide repeats (16). These tetratricopeptide repeats are required for the interaction of OGT with substrates (16). A missense mutation has also been identified in the tetratricopeptide repeat domain of OGT (L254F) that segregates with X-linked intellectual disability in a family (17). Moreover, it has been reported that mOGT regulated mitochondrial structure, function and cell survival (18). Using mOGT-specific siRNA in HeLa cells, reduced mOGT expression led to Drp1-dependent mitochondrial fragmentation, reduction in mitochondrial membrane potential and a significant loss of mitochondrial content in the absence of mitochondrial reactive oxygen species (ROS) (18).

In recent years, it has been reported that O-GlcNAcylation plays a variety of roles in both normal cellular processes and disease states. It regulates many fundamental cellular processes such as transcription, epigenetic modifications and cell signaling dynamics. Many studies have demonstrated that transcription factors are modified through O-GlcNAcylation. These include NFATC1, NF-κB, FOXO1, CRTC2, SP1, PGC1α, Pol II and a variety of other non-histone proteins (19–25). This indicates that OGT and O-GlcNAcylation are involved in transcriptional regulation.

Furthermore, epigenetic regulation, an important aspect of gene expression regulation, is closely associated with O-GlcNAcylation (26). O-GlcNAcylation is considered part of the histone code hypothesis which postulates that the PTMs to histones function as a signal platform to regulate specific chromatin functions (27). Indeed, previous research suggests that all four core histones (H2A, H2B, H3, H4) are modified by O-GlcNAcylation at Ser or Thr residues, and some have affirmed explicit functions (28–35). OGT also partners with many epigenetic regulators (36,37). For example, ten-eleven translocations (TETs) proteins function to recruit OGT to the chromatin and are associated with the O-GlcNAcylation of histones (38,39). In addition, it has been reported that OGT interacts with many epigenetic regulators such as HCF1, SIN3A complex, polycomb complex, etc. (40–45). In recent years, the evidence for a crosslink between epigenetic regulation and O-GlcNAcylation in tumor progression has gradually become stronger (26). Many reports have indicated that OGT and O-GlcNAcylation play an influential role in tumorigenesis and metastasis (5). However, the mechanism of this relationship is still unclear.

The nucleosome remodeling and deacetylase (NuRD) complex is a multisubunit complex containing nucleosome remodeling and histone deacetylase activities (46). The NuRD complex plays a significant role in many processes such as transcription, chromatin assembly, cell cycle progression and genomic stability (47,48). We have reported previously that the NuRD complex is involved in gene regulation and tumor invasion (49,50).

In this study, many previously undiscovered OGT-interacting proteins in multiple macromolecular complexes were identified by mass spectrum analysis. Additionally, an association between OGT and some epigenetic regulators, in particular the NuRD complex, was verified. Here, we present the first proteomic characterization of the protein–protein interaction (PPI) network of OGT as well as its regulatory targets. Our data indicate that OGT promotes the metastasis of cervical cancer, suggesting that OGT is an attractive target for cancer therapy.

Materials and methods

Cell culture and transfection

All cell lines used were obtained from the American Type Culture Collection. All cell lines were authenticated by short tandem repeat analysis in 2017. HeLa cells were maintained in Dulbecco's modified Eagle's medium. Ca Ski cells were maintained in RPMI-1640 medium. All media were supplemented with 10% fetal bovine serum, 100 units/ml penicillin and 100 mg/ml streptomycin (Gibco, BRL, Gaithersburg, MD). Cells were maintained in a humidified incubator equilibrated with 5% CO_2 at 37°C. Transfections were carried out using Lipofectamine® 2000 Reagent or Lipofectamine® RNAiMAX Reagent (Invitrogen, Carlsbad, CA) and TurboFect Transfection Reagent (Thermo Scientific) according to the manufacturer's instructions.

Antibodies and reagents

The sources of the antibodies were anti-FLAG, anti-HDAC1 anti-HDAC2, anti-RbAp46/48, anti-Fibronectin, anti-Vimentin and anti-β-actin (Sigma–Aldrich); anti-DDB1, anti-MTA1, anti-SIN3A, anti-SAP180 and anti-SAP30 (Santa Cruz Biotechnology); anti-PRMT5, anti-ROC1, anti-LSD1, anti-DNMT3B, anti-HDAC5 and anti-MTA2 (Abcam); anti-EED, anti-MBD2/3 and anti-MTA3 (Millipore); anti-SUZ12 (Cell Signaling Technology); anti-WDR77 (also known as MEP50, Bethyl); anti-MTA2, anti-E-cadherin, anti-α-catenin, anti-γ-catenin, anti-N-cadherin and anti-EZH2 (BD Bioscience); anti-ING4 (Genetex), anti-SETD2 (Proteintech). Dynabeads Protein G was obtained from Invitrogen by Thermo Fisher Scientific, and protease inhibitor mixture cocktail was from Roche Applied Science. Glutathione-Sepharose 4B beads were from GE Healthcare Bio-Sciences. Short hairpin RNAs (shRNAs) were obtained from GenePharma Co Ltd (Shanghai, China).

Cloning

FLAG–OGT plasmid was generated by inserting full-length OGT sequence into pCMV-Tag2B vector. Glutathione S-transferase (GST)–NuRD plasmids were created by inserting full-length NuRD components into pGEX-4T-3 expression vectors as described previously (50).

Immunopurification and mass spectrometry

HEK 293T cells stably expressing FLAG-tagged OGT were generated by transfection of the cells with FLAG-tagged OGT and selection in medium containing 1 mg/ml of G418 (Abcam). Anti-FLAG immunoaffinity columns were prepared using anti-FLAG M2 affinity gel (Sigma–Aldrich) following the manufacturer's suggestions. Cell lysates were obtained from approximately 5×10^8 cells and applied to an equilibrated FLAG column of 1 ml bed volume to allow for adsorption of the protein complex by the column resin. After binding, the column was then washed and followed by elution with FLAG peptides (Sigma–Aldrich). Fractions of the bed volume were collected, resolved on SDS-PAGE and silver stained. Gel bands then underwent liquid chromatography tandem mass spectroscopy sequencing and analysis.

Immunoprecipitation and western blotting

For immunoprecipitation (IP) assays, cells were washed with cold phosphate-buffered saline (PBS) and lysed with cold cell lysis buffer for 30 min at 4°C. Five hundred micrograms of cellular extracts were incubated with appropriate specific antibodies or normal rabbit/mouse immunoglobin G at 4°C overnight with constant rotation, followed by addition of protein Glutathione-Sepharose beads for 2 h at 4°C. Beads were then washed five times with cell lysis buffer (50 mM Tris–HCl, pH 7.4, 150 mM NaCl, 1 mM

EDTA, 0.5% NP-40, 0.25% sodium deoxycholate and protease inhibitor mixture). The immune complexes were subjected to SDS-PAGE followed by immunoblotting (IB) with secondary antibodies. Immunodetection was performed using enhanced chemiluminescence (ECL System, Thermo Scientific) according to the manufacturer's instructions.

GST pull-down experiments

GST fusion constructs were expressed in BL21 *Escherichia coli* cells, and crude bacterial lysates were prepared by sonication in cold PBS in the presence of protease inhibitor mixture. The *in vitro* transcription and translation experiments were performed with rabbit reticulocyte lysate (TNT Systems; Promega). In GST pull-down assays, approximately 10 μg of the appropriate GST fusion proteins were mixed with 5–8 μl of the *in vitro* transcribed/translated products and incubated in binding buffer (0.8% BSA in PBS in the presence of the protease inhibitor mixture). The binding reaction was then added to 30 μl of Glutathione-Sepharose beads and mixed at 4°C for 2 h. The beads were washed five times with binding buffer, resuspended in 30 μl of 2× SDS-PAGE loading buffer and resolved on 12% gels. Protein bands were detected with specific antibodies using western blot analysis.

Chromatin immunoprecipitation and quantitative chromatin immunoprecipitation

Chromatin immunoprecipitations (ChIPs) and quantitative chromatin immunoprecipitations (qChIPs) were performed using HeLa cells as described previously (49). Briefly, 1×10^7 cells were cross-linked with 1% formaldehyde, sonicated, precleared and incubated with 5–10 μg of antibody per reaction. Complexes were washed with low and high salt buffers, and the DNA was extracted for qChIP assay. The primers used are listed in Supplementary File S2, available at *Carcinogenesis* Online.

RT-PCR and qPCR

Total cellular RNA was extracted from HeLa cells infected by concentrated virus expressing shOGT or shSCR control with TRIzol according to the manufacturer's instructions (Invitrogen). Potential DNA contamination was mitigated using RNase-free DNase treatment (Promega). cDNA was prepared with the MMLV Reverse Transcriptase (Promega). Briefly, cDNA was mixed with 1 μl forward and reverse primers (5 μM of each), 8 μl RNase-free water and 10 μl 2× PCR SYBR Green Mix buffer in a 20 μl reaction. Forty cycles of PCR were conducted at 95°C for 15 s and 60°C for 1 min within each cycle. Relative quantitation was determined utilizing the ABI PRISM 7500 sequence detection system (Applied Biosystems, Foster City, CA) through the measurement of real-time SYBR green fluorescence, and the results were obtained by means of the comparative Ct method ($2^{-\Delta\Delta Ct}$) using glyceraldehyde 3-phosphate dehydrogenase as an internal control. This experiment was performed in triplicate. The primers used are listed in (Supplementary File S2, available at *Carcinogenesis* Online).

Lentiviral production and infection

Recombinant lentiviruses expressing shOGT was constructed by Shanghai GenePharma. Concentrated viruses were generated and infected 5×10^5 cells in a 60 mm dish with 8 μg/ml polybrene. Infected cells were then subject to sorting target expression. The shRNA sequences are listed in Supplementary File S2, available at *Carcinogenesis* Online.

Cell invasion assay

Transwell chamber filters (Becton Dickinson) were coated with Matrigel. After infection with lentivirus, cells were suspended in serum-free media, and 3×10^4 cells in 0.5 ml serum-free media were placed into the upper chamber of the transwell. The chamber was then transferred to a well containing 500 μl of media containing 10% fetal bovine serum. Cells were incubated for 18 to 24 h at 37°C. Cells in the top well were removed by wiping the top of the membrane with cotton swabs. The membranes were then stained, and the remaining cells were counted. Three high-powered fields were counted for each membrane.

Wound healing assay

Wound healing assay was carried out to determine the cell migration ability of tumor cells. After infection with lentivirus, cells were seeded into six-well dishes and grown for 24 h to 80–90% confluence. A linear wound was generated by scratching the subconfluent cell monolayer using a pipette tip (200 μl, Axygen), and the debris was removed by washing with PBS. Migration of cells into the wound was then observed every 4 h. After incubation at 37°C for 48 h, the migration of the cells toward the wound was photographed under a light microscope. Then the relative migration rate was calculated. Experiments were carried out at least three times.

Results

Proteomic analysis of the OGT interactomes

In an effort to better understand the mechanistic role of OGT, affinity purification and mass spectrometry assays were used to identify the proteins that are associated with OGT *in vivo* (Figure 1A). In these experiments, FLAG-tagged OGT or an empty vector was stably expressed in HeLa cells. Cellular extracts were prepared and subjected to affinity purification using an anti-FLAG affinity gel. Immunocomplex proteins were separated using SDS-PAGE and silver stained (Figure 1B). Immunoprecipitated proteins in 14 specific bands in comparison with the vector were gel extracted, trypsin digested and identified using liquid chromatography tandem mass spectroscopy. Surprisingly, >1200 unique proteins with a protein score equal to or higher than two were identified (Supplementary File S1, available at *Carcinogenesis* Online). These proteins were then classified into various cellular signaling pathways using Kyoto Encyclopedia of Genes and Genomes (KEGG) pathway software (http://www.kegg.jp/kegg/pathway.html; Figure 1C). Further analysis showed that these signaling pathways were involved not only in many physiological processes but also the pathogenesis of many diseases including cancer.

To identify putative functional processes associated with OGT-interacting proteins, we performed Gene Ontology (GO) analysis (Figure 1D–F). The top-ranked categories of Biological Process (BP) analysis were gene expression, RNA metabolic process, chromosome organization, translation and so on, suggesting that OGT is related to gene transcriptional regulation and expression. In addition, Molecular Function (MF) analysis identified many predominant themes including nucleic acid binding, chromatin binding, histone binding, etc. This indicates that OGT may be involved in epigenetic regulation such as DNA/RNA or histone modification and chromatin remodeling. Cellular Component (CC) analysis showed that OGT-interacting proteins were related to nucleoplasm, nucleolus, chromosomes, anchoring junction, adherens junction and cell junction, which implies that OGT is likely to participate in cell adhesion and invasion.

To further research the functional relationship between the OGT-interacting proteins and identify specific functional complexes, a PPI network of the identified proteins was constructed using the STRING online database (http://string-db.org; Figure 1G). PPI analysis revealed multiple OGT-associated complexes which suggest previously unknown functions of OGT. For example, we identified many functional proteins associated with histone methylation and acetylation (important histone modification processes), polycomb group proteins (well known for Hox gene silencing), writers and erasers of ubiquitination modification and many functional proteins associated with DNA methylation. Notably, the PPI analysis identified nearly every component of the NuRD complex, which is important in histone deacetylation and chromatin remodeling. The selected OGT-interacting epigenetic regulatory proteins are listed in Table 1.

OGT is physically associated with the NuRD complex

To confirm the *in vivo* interaction between OGT and the interacting proteins, total proteins from HeLa cells were extracted and co-IP was performed with antibodies detecting the endogenous

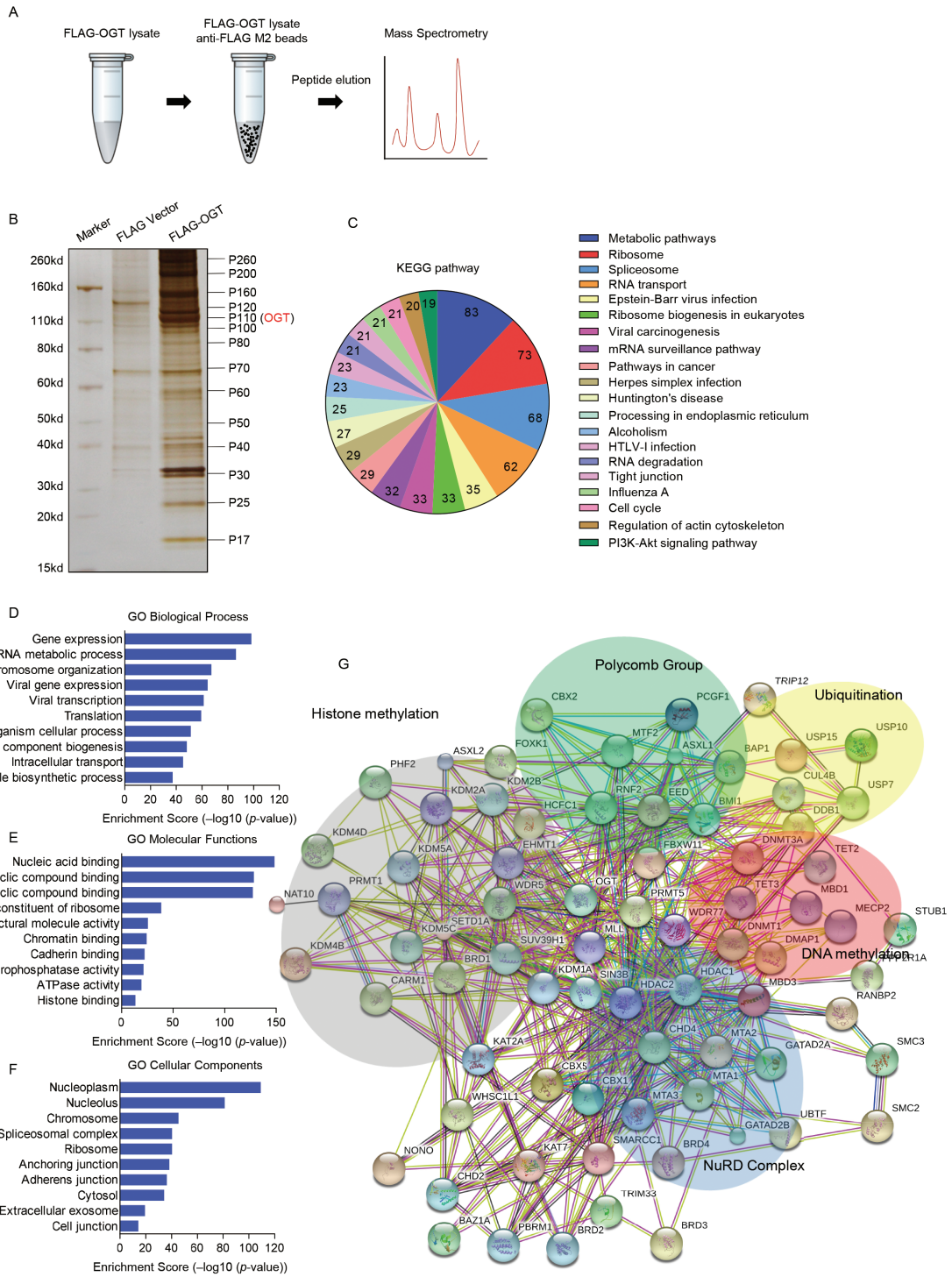

Figure 1. Proteomic analysis of the OGT interactomes. (**A**) The affinity purification and mass spectrometry approach used in this study. (**B**) Immunoaffinity purification of OGT-containing protein complexes. Cellular extracts from HEK 293T cells stably expressing FLAG (control) or FLAG-OGT were immunopurified with anti-FLAG affinity columns and eluted with FLAG peptide. The eluates were resolved using SDS-PAGE and silver stained. The protein bands were retrieved and analyzed using mass spectrometry. Detailed results from the mass spectrometry analysis are provided in Supplementary File S1, available at *Carcinogenesis* Online. (**C**) KEGG pathway analysis of the OGT-interacting proteins categorized into functional groups. (**D**–**F**) GOs analysis of OGT-interacting proteins. (**G**) PPI analysis of OGT-associated proteins.

proteins. IP with antibodies against OGT followed by IB with antibodies against PRMT5, MEP50, EZH2, SUZ12, EED, BMI1, SIN3A, SAP180, SAP30, CUL4B, DDB1, ROC1, TET1/2/3, WDR5 and USP7 demonstrated that these proteins were efficiently coimmunoprecipitated with OGT (Figure 2A).

As mentioned above, almost every component of the NuRD complex had been identified in the mass spectroscopy results. IP with antibodies against OGT followed by IB with antibodies against components of the NuRD complex demonstrated that they were efficiently coimmunoprecipitated with OGT.

Table 1. Detailed results for the focused OGT-interacting proteins involved in PPI analysis

Gene symbol	Peptides (coverage %)	Annotation	Gene symbol	Peptides (coverage %)	Annotation	Gene symbol	Peptides (coverage %)	Annotation
OGT	74 (71.99)	O-GlcNAcylation	SMC2	25 (21.14)		CHD2	13 (7.76)	
PRMT5	37 (52.9)	Histone methylation	CBX2	8 (21.05)	Polycomb group	MTA1	3 (6.85)	NuRD complex
BRD2	31 (42.82)		PBRM1	34 (20.92)		SUV39H1	3 (6.8)	Histone methylation
PPP2R1A	17 (41.95)		WDR5	4 (20.66)	Histone methylation	KDM5A	10 (6.66)	Histone methylation
CBX5	7 (41.36)		UBTF	13 (19.81)	Ubiquitination	MBD1	3 (6.56)	DNA methylation
RNF2	10 (40.48)	Polycomb group	SETD1A	29 (19.63)	Histone methylation	KAT2A	2 (6.52)	Acetylation
NONO	21 (38.64)		MTF2	8 (19.22)	Polycomb group	KDM4D	3 (6.12)	Histone methylation
STUB1	11 (38.28)	Ubiquitination	BMI1	6 (19.02)	Ubiquitination Polycomb group	FBXW11	3 (5.91)	Ubiquitination
CBX1	8 (37.57)		GATAD2B	8 (18.04)	NuRD complex	KDM4B	2 (5.8)	Histone methylation
HDAC2	14 (35.59)	NuRD complex Acetylation	PCGF1	4 (17.61)	Polycomb group	TRIM33	4 (5.67)	
HDAC1	15 (35.06)	NuRD complex Acetylation	DNMT3A	15 (17.21)	DNA methylation	NSD3	6 (5.09)	Histone methylation
WDR77	11 (34.8)	Histone methylation	MBD3	4 (16.22)	NuRD complex	USP15	5 (4.79)	Ubiquitination
DDB1	31 (34.04)	Ubiquitination	BRD3	10 (15.98)		FOXK1	4 (4.5)	
MECP2	13 (33.54)	DNA methylation	SMARCC1	16 (14.84)		USP10	3 (4.39)	Ubiquitination
PRMT1	9 (32.92)	Histone methylation	BRD1	16 (13.71)		ASXL2	5 (4.34)	
NAT10	31 (32.68)	Acetylation	CUL4B	9 (12.97)	Ubiquitination	TET2	7 (3.8)	DNA methylation
BAZ1A	49 (31.49)		CARM1	5 (12.5)	Histone methylation	EHMT1	5 (3.62)	Histone methylation
MTA2	17 (31.44)	NuRD complex	BAP1	8 (12.35)	Ubiquitination Polycomb group	ASXL1	5 (3.39)	Polycomb group
HCFC1	40 (28.8)		KDM1A	11 (12.32)	Histone methylation	PHF2	3 (3.1)	Histone methylation
SMC3	32 (28.27)		MTA3	5 (11.28)	NuRD complex	USP7	3 (2.99)	Ubiquitination
DMAP1	10 (27.62)	DNA methylation	TRIP12	17 (10.74)		KDM5C	4 (2.68)	Histone methylation
EED	9 (26.5)	Polycomb group Histone methylation	KDM2A	11 (10.59)	Histone methylation	SIN3B	3 (2.65)	Acetylation
KAT7	10 (22.75)	Acetylation	RANBP2	24 (9.46)		KMT2A	5 (1.58)	Histone methylation
GATAD2A	10 (22.04)	NuRD complex	DNMT1	12 (8.83)	DNA methylation	TET3	2 (1.51)	DNA methylation
CHD4	39 (21.21)	NuRD complex	BRD4	13 (8.52)		KDM2B	1 (0.95)	Histone methylation

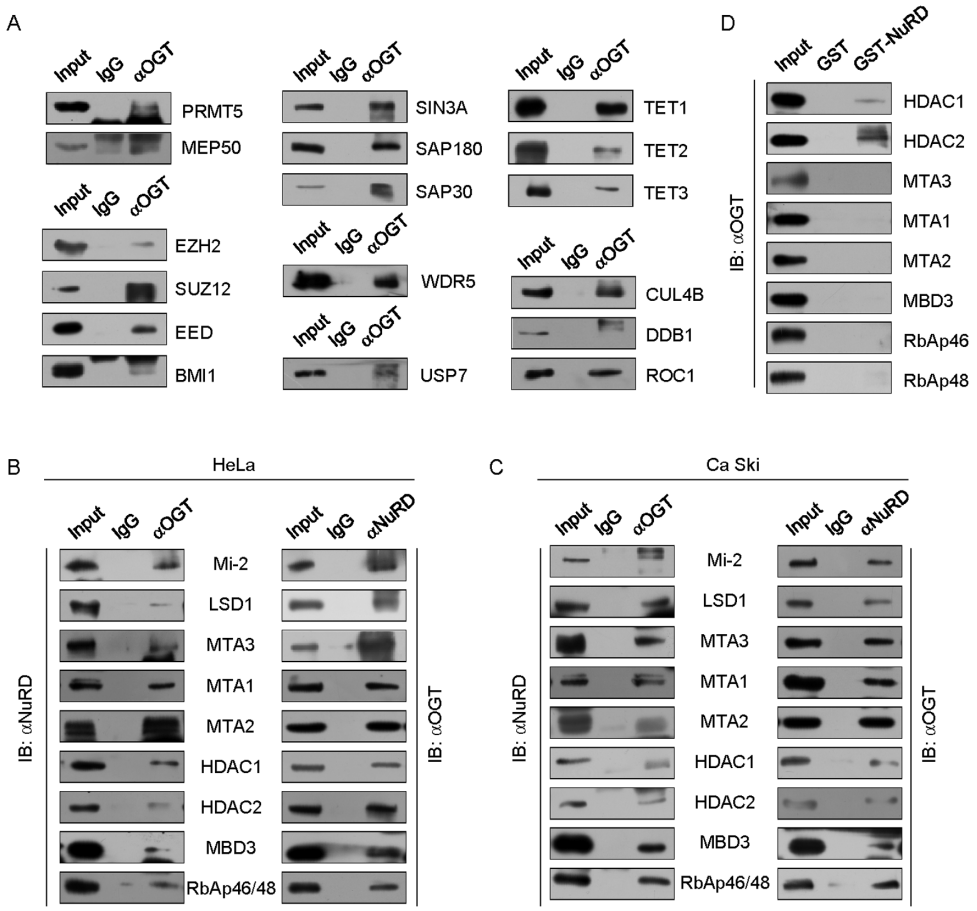

Figure 2. OGT is physically associated with the NuRD complex. (**A**)Whole cell lysates from HeLa cells were prepared, and co-IP was performed with antibodies against OGT. Immunocomplexes were then IB tested using antibodies against the indicated proteins. IgG served as the negative control. (**B** and **C**) Association of OGT with the NuRD complex in HeLa cells and Ca Ski cells. Whole cell lysates were immunoprecipitated with antibodies against the indicated proteins. Immunocomplexes were then IB tested using antibodies against the indicated proteins. (**D**) Molecular interaction between OGT and the NuRD complex. GST pull-down experiments with bacterially expressed GST-fused proteins and *in vitro* transcribed/translated OGT.

Reciprocally, IP with antibodies against representative components of the NuRD complex and IB with antibodies against OGT reinforced the finding that OGT was efficiently coimmunoprecipitated with the NuRD complex components (Figure 2B). Associations between OGT and the NuRD complex were also detected in Ca Ski cells (Figure 2C).

In order to further explore the molecular basis for the interaction between OGT and the NuRD complex, GST pull-down assays were performed using GST-fused components of the NuRD complex and *in vitro* transcribed/translated OGT. These experiments revealed that OGT could interact directly with HDAC1/2 (Figure 2D).

Genome-wide identification of transcriptional targets for OGT

As described above, the GO analysis of OGT-interacting proteins demonstrated that OGT was involved in gene transcriptional regulation and expression. To further investigate the biological significance of OGT and to explore its downstream target genes, we subsequently analyzed the genome-wide transcriptional targets of OGT using the RNA-seq approach. In these experiments, siRNA was used to knockdown the expression of OGT in HeLa cells. After RNA extraction, purification, reverse transcription and amplification, the DNA product was cyclized and sequenced. Three independent samples and controls (Control-1, Control-2, Control-3 and siOGT-1, siOGT-2, siOGT-3) were used in these experiments. After data analysis, the mRNA expression was clustered using Cluster 3.0 software and plotted in Figure 3A.

A scatter plot of all expressed genes is shown in order to identify the differentially expressed genes with a fold change ≥2 and divergence probability ≥0.8 (Figure 3B). We found 231 upregulated genes and 583 downregulated genes between the control groups and OGT knockdown groups. A volcano plot is also shown to identify these differentially expressed genes (Figure 3C).

To further explore the function of OGT in gene regulation, we analyzed the difference of gene expression in depth. The function of OGT was annotated using the GO and KEGG pathway analysis (Figure 3D and E). The results indicate that OGT is associated with regulation of many vital cell processes and activities. Moreover, the differentially expressed genes were analyzed by gene set enrichment analysis (GSEA) approach. We observed an enrichment of differentially expressed genes in many important processes such as epithelial–mesenchymal transition (EMT), p53 pathway, WNT signaling pathway, inflammatory response, transforming growth factor beta signaling pathway and apoptosis (Figure 3F).

For further investigation, we tested lentivirus-delivered shRNA packages targeted to OGT. Two efficient shRNAs were chosen for the following experiments. Consistent with the RNA-seq

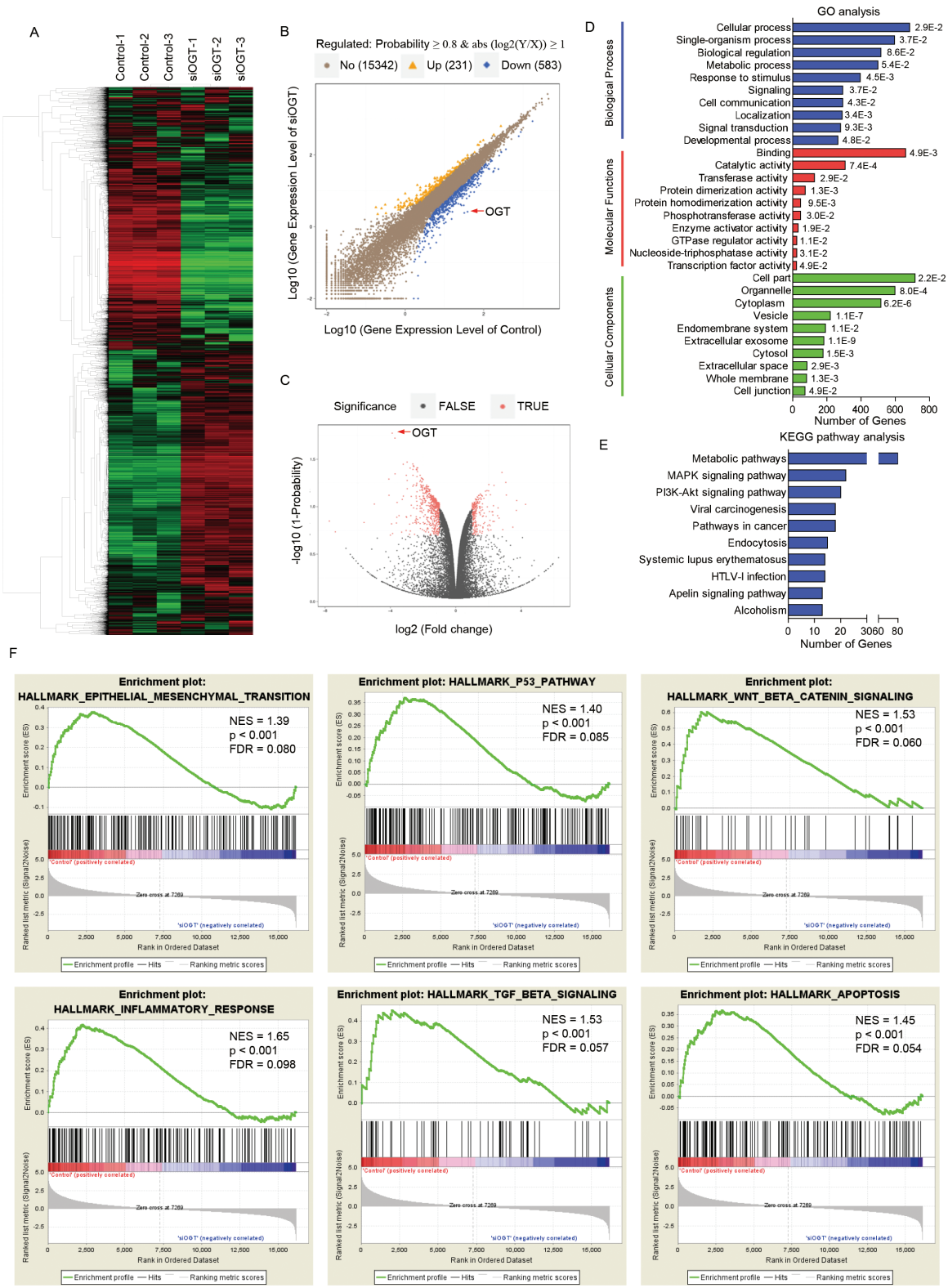

Figure 3. Genome-wide identification of transcriptional targets for OGT. (**A**) siRNA was used to knock down the expression of OGT in HeLa cells. Three independent samples were used in the RNA-seq analysis. mRNA expression data were clustered using Cluster 3.0 software. (**B**) Scatter plot of all expressed genes is shown to identify differentially expressed genes with fold change ≥2 and divergence probability ≥0.8. (**C**) Volcano plot is shown to identify the differentially expressed genes. (**D** and **E**) GO and KEGG pathway analysis of the difference of gene expression was performed to further explore the function of OGT in gene regulation. (**F**) GSEA analysis of the difference of gene expression.

results, knockdown of OGT in HeLa cells led to changed expression of many important genes at both the transcriptional level (Figure 4A and B) and the protein level (Figure 4C), as expected. Among these genes are Snail/SNAI1, a vital transcription factor that is closely related to EMT and cell invasion (51,52), and ING4, a tumor suppressor which is involved in the TP53-dependent regulatory pathway (53,54).

To investigate the function of OGT in transcriptional regulation, we performed quantitative ChIP analysis in HeLa cells using specific antibodies against OGT on the selected genes. The results showed that OGT was enriched on the promoters of *JMJD7*, *HDAC5*, *HLA*, *FBXW5*, *DNMT3B*, *FBXO4*, *MSH5*, *KMT5C* and *ING4* (Figure 4D).

OGT promotes EMT and invasion of cervical cancer cells

As stated previously, OGT-interacting proteins were observed to be related to the anchoring junction, adherens junction and cell junction, which implies that OGT is likely to participate in cell

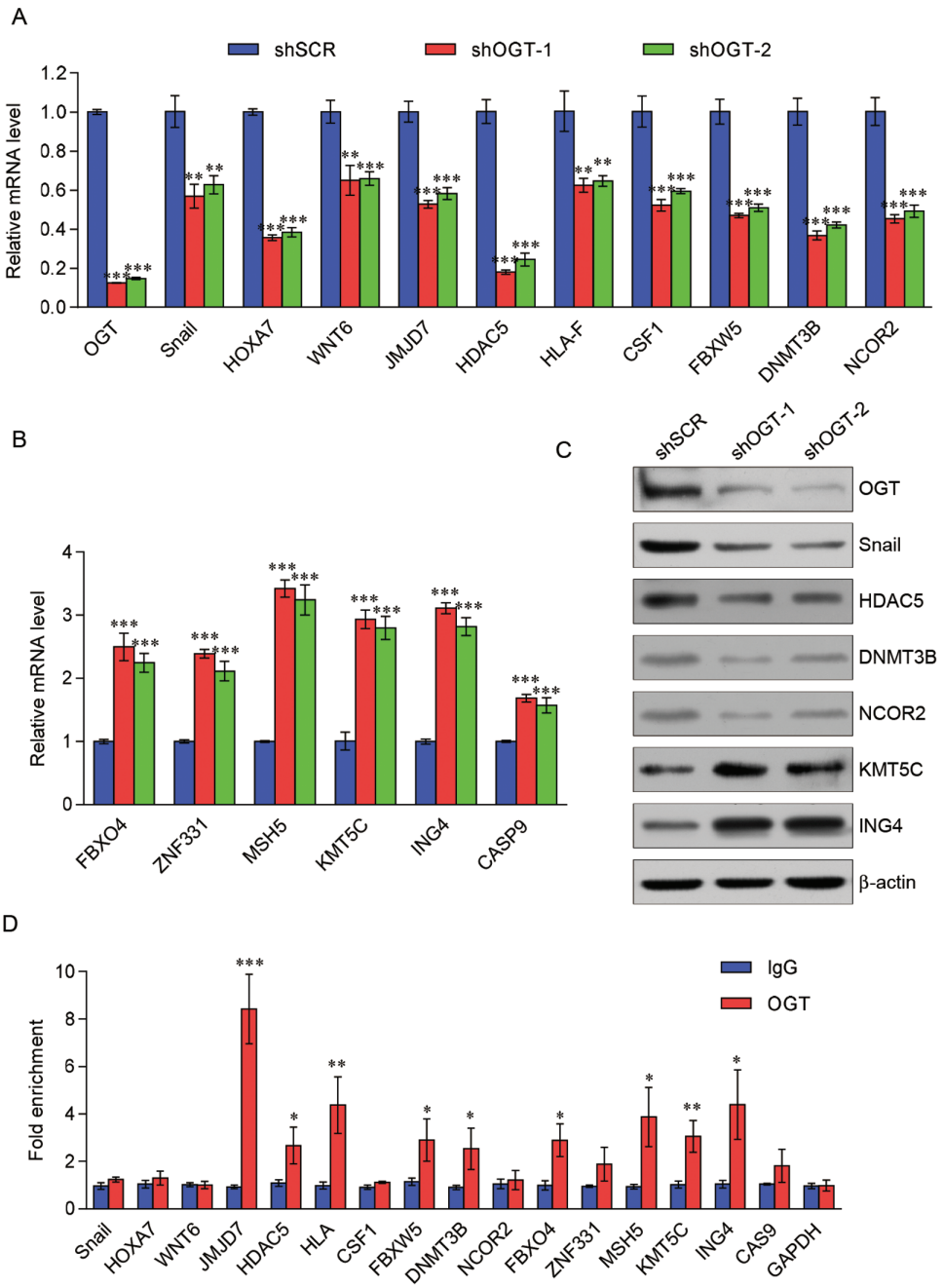

Figure 4. Validation of the transcriptional regulation of OGT on target genes. (**A–C**) HeLa cells were infected with lentivirus carrying shRNA (shSCR) or shRNAs targeting OGT and overexpression vectors. Real-time RT-PCR and western blot analyses of partial transcriptional target expression in HeLa cells infected with lentiviruses carrying the indicated shRNAs are shown. (**D**) qChIP analysis of the selected promoters was performed using antibodies against IgG and OGT. Results are represented as fold change over IgG with glyceraldehyde 3-phosphate dehydrogenase as a negative control. Error bars represent mean ± SD for three independent experiments (*$P < 0.05$, **$P < 0.01$, ***$P < 0.001$ and two-tailed unpaired *t*-test).

adhesion and invasion. Furthermore, the transcription factor Snail controls EMT and cell invasion, and ING4 is a vital tumor suppressor. We also found that knockdown of OGT resulted in altered expression of some EMT-related factors in the RNA-seq data (Figure 5A). Because of our findings, we subsequently investigated the specific role OGT plays in EMT and the invasion process of cervical cancer. To this end, we detected the expression level of some invasion markers of EMT under the influence of loss-of-function of OGT. qPCR and western blot analysis showed that the expression of some epithelial markers (α-catenin, γ-catenin and E-cadherin) increased whereas some mesenchymal markers (*N*-cadherin, Fibronectin and Vimentin) decreased (Figure 5B and C).

In order to investigate the function of OGT in cell migration and invasion, two cervical cancer cell lines (HeLa and Ca Ski) were used. We examined the cellular migration of HeLa and Ca Ski cells using an *in vitro* wound healing assay. We observed that the knockdown of OGT by two separate shRNAs resulted in a significant delay in wound closure compared with the control groups (Figure 5D). We then investigated the roles of OGT in cellular behavior of cervical cancer cells *in vitro* using transwell invasion assays. As shown in Figure 5E, knockdown of OGT led to a statistically significant decrease in the invasive potential of HeLa or Ca Ski cells, whereas overexpression led to a statistically significant increase in invasive potential ($P < 0.05$). Collectively, these results indicate that OGT promotes the invasion and migration potential of cervical cancer cells.

The expression of OGT is upregulated in cervical cancer and correlated with the expression of Snail and ING4

In order to further investigate the role of OGT in clinical samples of cervical cancer, we analyzed published data downloaded from the Oncomine database (https://www.oncomine.com/). We found that the expression of OGT was upregulated in cervical cancer compared with adjacent normal tissues (Figure 6A). Analysis of two published clinical datasets (GSE3578 and GSE6213) from the GEO database (http://www.ncbi.nlm.nih.gov/geo/) revealed that the expression of Snail was statistically significantly positively correlated with the expression of OGT ($P < 0.05$) and that expression of ING4 was negatively correlated with expression of OGT ($P < 0.05$), which supports our findings that Snail and ING4 are downstream target genes of OGT (Figure 6B). To extend our observations to a clinical pathologically relevant context, we analyzed the expression of OGT and its correlation with clinical behaviors of cancer patients. Kaplan–Meier survival analysis of OGT performed with the online tool (http://kmplot.com/analysis/) (55) showed that lower expression of OGT was associated with improved survival in cancer patients, when the influence of systemic treatment, endocrine therapy and chemotherapy was excluded (Figure 6C).

Discussion

Our data indicate that OGT interacts with multiple types of proteins. As we have shown, using KEGG pathway and GO analysis, OGT-associated proteins were involved in many kinds of vital signaling pathways and biological processes, which indicates the importance and multifunctionality of OGT and *O*-GlcNAcylation. These results have convinced us that many of the interacting proteins are substrates of OGT. Among those identified by our mass spectroscopy results, many *O*-GlcNAcylated proteins have been reported previously such as CARM1 (56), SETD1A (39), HAT (57), HDAC (58), TET family (59–61), EZH2 (62) and so on. On the other hand, some proteins were observed as interacting with, but not *O*-GlcNAcylated by OGT. For instance, OGT coordinates with some epigenetic regulators to modify histones since *O*-GlcNAcylation is admitted as a new kind of histone code.

NuRD complex is one of the epigenetic regulators that we found interacted with OGT. NuRD is a multicomponent complex which contains not only adenosine triphosphate-dependent nucleosome disruption activity but also histone deacetylase activity (63). We first reported, here, that OGT was associated with the NuRD complex and directly associated with HDAC1 and HDAC2. However, the effect of this association remains unclear. We speculate that one or more components may be substrates of *O*-GlcNAcylation. Alternatively, OGT may coordinate with the NuRD complex to participate in histone modification and chromatin remodeling. We will investigate this possibility in follow-up studies.

In addition to the interacting proteins, we also focused on downstream target genes of OGT by RNA-seq approach. We identified many differentially expressed genes including *Snail* and *ING4*. Snail is a zinc-finger transcription factor (64). It is an important transcription repressor which is involved in the EMT process through the repression of E-cadherin (51,52). We have demonstrated that Snail is a downstream target of OGT. Coincidentally, it has been reported that Snail is regulated by the MTA3/NuRD complex (65). It is of interest that OGT and the NuRD complex may coordinately regulate the expression of Snail.

Another important downstream target of OGT is ING4, which is a member of the inhibitor of growth (ING) family. The ING family consists of five evolutionarily conserved proteins (ING1–5), which function as type II tumor suppressors (66,67). ING family proteins have also been implicated in various critical cellular processes, such as cell proliferation, apoptosis, DNA repair, senescence, angiogenesis and drug resistance (53,68). Moreover, ING4 can physically interact with p300 and p53 *in vivo* and can also enhance p53 acetylation at Lys-382 (54). It is reported that downregulation of ING4 is correlated with high-grade tumors and poor prognosis, suggesting that ING4 plays an important role in tumor initiation and metastasis (69,70). It is important to know how the ING4 protein is regulated in a normal or tumorigenic environment. Our colleagues have demonstrated that JFK targets ING4 for ubiquitination and degradation through assembly of an Skp1–Cul1–F-box complex, which has been found to lead to hyperactivation of the canonical NF-κB pathway and promote angiogenesis and metastasis of cancer (71). We have reported that ING4 is a downstream target of OGT, and the expression level of ING4 is negatively correlated with OGT levels. Further investigations are warranted to determine the molecular mechanism by which OGT regulates ING4. The other interacting proteins or downstream targets of OGT also deserve further study.

In view of the important roles of NuRD complex, Snail and ING4 in EMT and cancer metastasis, we have reasons to believe that OGT and *O*-GlcNAcylation are also involved in tumor progression. There is no doubt that cancer is not only a genetic disease but it also occurs due to epigenetic abnormalities (72). It is known that aberrant epigenetic regulation of gene expression contributes to different stages of cancer development and resistance to chemotherapy (73). In recent years, studies have revealed that diet and environmental factors can alter the scope of epigenetic regulation (74–77). Recent studies have suggested that *O*-GlcNAcylation, which involves the addition of

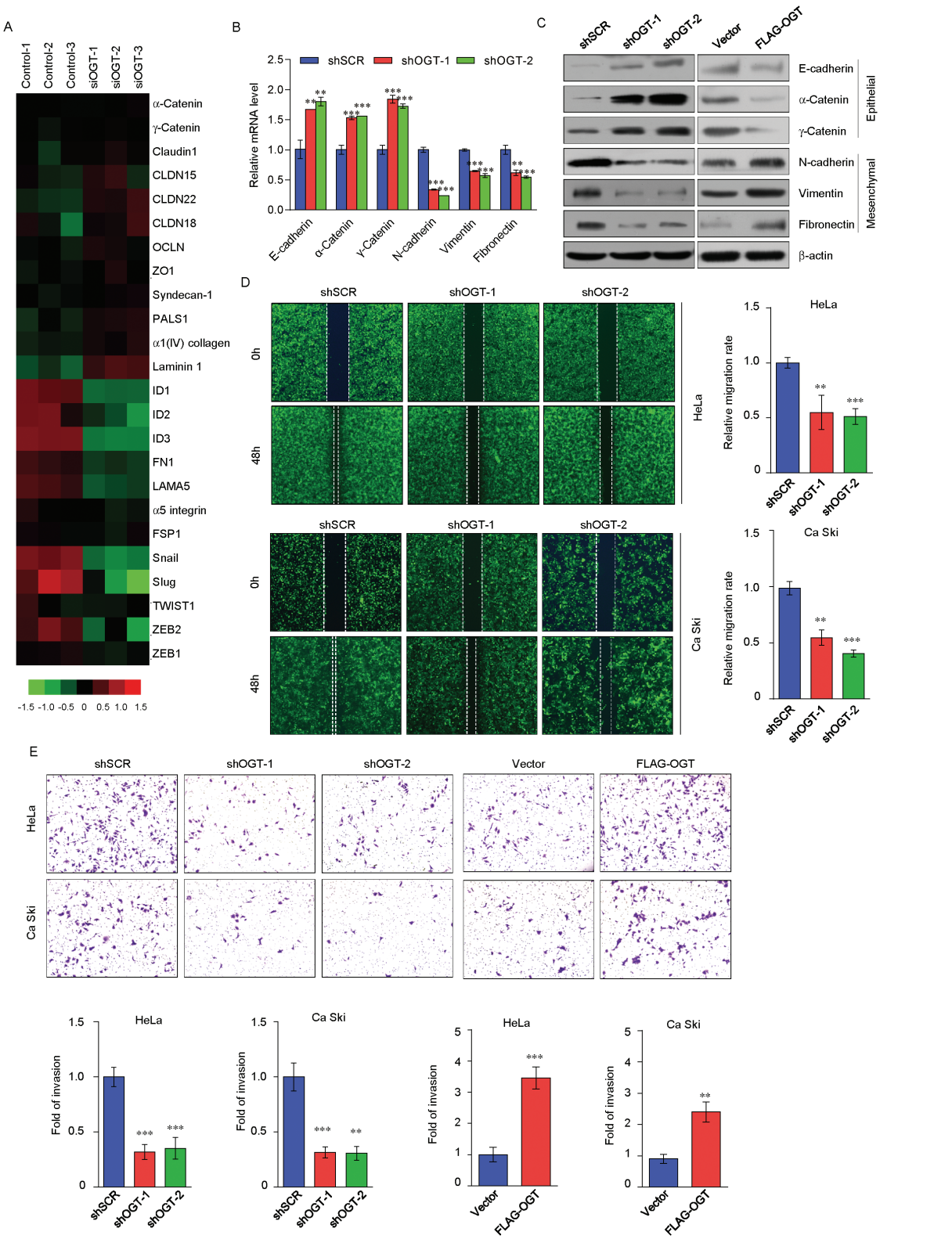

Figure 5. OGT promotes the EMT and invasion of cervical cancer cells. (**A**) Analysis of the expression of EMT-related factors. (**B** and **C**) The expression of the indicated epithelial or mesenchymal markers was measured using real-time RT-PCR (B) or western blotting (C) in HeLa cells infected with lentiviruses carrying the indicated shRNAs or overexpressing OGT. (**D**) HeLa cells and Ca Ski cells were transfected with lentivirus-shOGT. After a linear wound was generated, cells were incubated at 37°C for 48 h in six-well dishes. The migration of cells toward the wound was photographed under a light microscope. Subsequently, relative migration rates were calculated. The images represent one of the three photographed wells in each group. (**E**) HeLa cells and Ca Ski cells were transfected with lentivirus-shOGT or FLAG-OGT for cell invasion assays using Matrigel transwell filters. The invaded HeLa and Ca Ski cells transfected with shOGT were stained and counted 24 h after seeded, with the cells transfected with FLAG-OGT for 18 h. The images represent one field under microscopy in each group. Error bars represent mean ± SD for three independent experiments (*$P < 0.05$, **$P < 0.01$, ***$P < 0.001$ and two-tailed unpaired *t*-test).

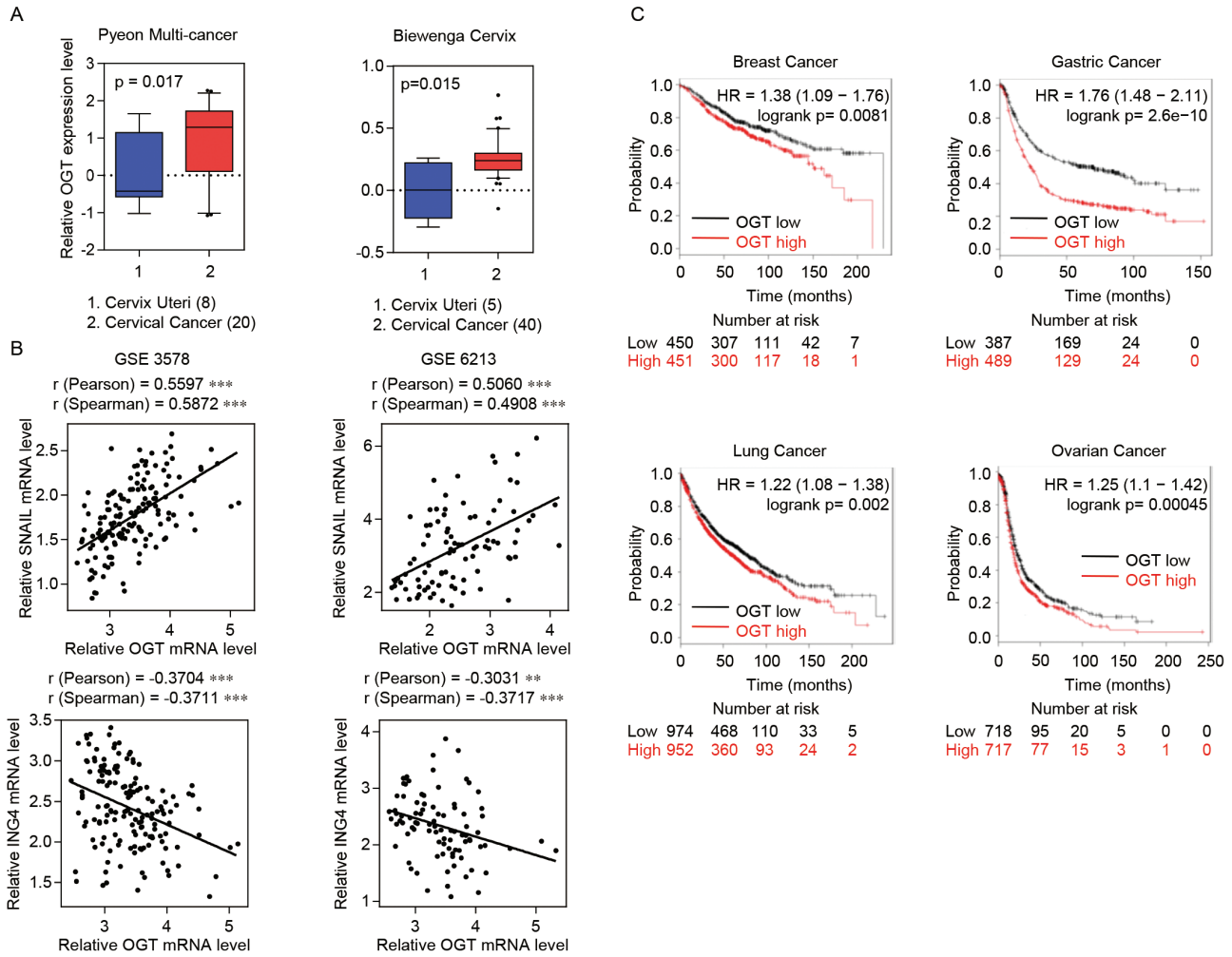

Figure 6. The expression of OGT is upregulated in cervical cancer and correlated with the expression of Snail and ING4. (**A**) The OGT expression in cervical cancer microarray datasets available from Oncomine (https://www.oncomine.com/). (**B**) Analysis of public datasets (GSE3578 and GSE6213) for the expression of OGT and Snail/ING4 in cervical cancer. The relative levels of Snail/ING4 were plotted against that of OGT. (**C**) Kaplan-Meier survival analysis for the relationship between survival time and *OGT* signature in breast cancer, gastric cancer, lung cancer and ovarian cancer using the online tool (http://kmplot.com/analysis/).

N-acetylglucosamine on the serine or threonine residues of proteins, may play an important role in the regulation of the epigenome in response to the metabolic status of the cell. OGT, which catalyzes the addition of the GlcNAc moiety to target proteins, has been shown to play an influential role in tumorigenesis and metastasis (5). It has been reported that human papillomavirus E6 upregulates OGT, increases O-GlcNAc, stabilizes c-MYC via O-GlcNAc and enhances human papillomavirus oncogene activities in cervical cancer (78). All these pieces of evidence suggest that aberrant glucose metabolism may be a risk factor for cervical cancer and resistance to chemotherapy, which offers a promising avenue of further study for the development of cervical cancer drugs.

In summary, our experiments have revealed multiple novel and unexpected physiological functions of OGT using proteomic analysis and target analysis. Our study has uncovered a conceivable mechanism by which OGT influences the EMT process and tumor invasion through regulation of Snail. Our work supported the pursuit of OGT as a target for cancer intervention.

Supplementary material

Supplementary Files 1 and 2 can be found at *Carcinogenesis* online.

Funding

This work was supported by grant (2016YFA0102400 to Y.W.) from the Major State Basic Research Development Program of China, grants (81773017 and 81472733 to Y.W., 81402334 to Y.Y., 81502446 to R.Q.) from National Natural Science Foundation of China.

Conflict of Interest Statement: None declared.

References

1. Hart, G.W. *et al.* (2007) Cycling of O-linked beta-N-acetylglucosamine on nucleocytoplasmic proteins. Nature, 446, 1017–1022.
2. Love, D.C. *et al.* (2005) The hexosamine signaling pathway: deciphering the "O-GlcNAc code". Sci. STKE., 2005, re13.
3. Hart, G.W. *et al.* (2011) Cross talk between O-GlcNAcylation and phosphorylation: roles in signaling, transcription, and chronic disease. Annu. Rev. Biochem., 80, 825–858.
4. Yi, W. *et al.* (2012) Phosphofructokinase 1 glycosylation regulates cell growth and metabolism. Science, 337, 975–980.
5. Slawson, C. *et al.* (2011) O-GlcNAc signalling: implications for cancer cell biology. Nat. Rev. Cancer, 11, 678–684.
6. Yang, X. *et al.* (2008) Phosphoinositide signalling links O-GlcNAc transferase to insulin resistance. Nature, 451, 964–969.
7. Ruan, H.B. *et al.* (2013) Cracking the O-GlcNAc code in metabolism. Trends Endocrinol. Metab., 24, 301–309.

8. Yuzwa, S.A. *et al.* (2012) Increasing O-GlcNAc slows neurodegeneration and stabilizes tau against aggregation. Nat. Chem. Biol., 8, 393–399.
9. Liu, R. *et al.* (2017) MicroRNA-15b suppresses Th17 differentiation and is associated with pathogenesis of multiple sclerosis by targeting O-GlcNAc transferase. J. Immunol. 198, 2626–2639.
10. Gao, Y. *et al.* (2001) Dynamic O-glycosylation of nuclear and cytosolic proteins: cloning and characterization of a neutral, cytosolic beta-N-acetylglucosaminidase from human brain. J. Biol. Chem., 276, 9838–9845.
11. Shafi, R. *et al.* (2000) The O-GlcNAc transferase gene resides on the X chromosome and is essential for embryonic stem cell viability and mouse ontogeny. Proc. Natl. Acad. Sci. USA, 97, 5735–5739.
12. O'Donnell, N. *et al.* (2004) Ogt-dependent X-chromosome-linked protein glycosylation is a requisite modification in somatic cell function and embryo viability. Mol. Cell. Biol., 24, 1680–1690.
13. Jínek, M. *et al.* (2004) The superhelical TPR-repeat domain of O-linked GlcNAc transferase exhibits structural similarities to importin alpha. Nat. Struct. Mol. Biol., 11, 1001–1007.
14. Lazarus, M.B. *et al.* (2011) Structure of human O-GlcNAc transferase and its complex with a peptide substrate. Nature, 469, 564–567.
15. Olszewski, N.E. *et al.* (2010) O-GlcNAc protein modification in plants: evolution and function. Biochim. Biophys. Acta, 1800, 49–56.
16. Yang, X. *et al.* (2017) Protein O-GlcNAcylation: emerging mechanisms and functions. Nat. Rev. Mol. Cell Biol., 18, 452–465.
17. Vaidyanathan, K. *et al.* (2017) Identification and characterization of a missense mutation in the O-linked β-N-acetylglucosamine (O-GlcNAc) transferase gene that segregates with X-linked intellectual disability. J. Biol. Chem., 292, 8948–8963.
18. Sacoman, J.L. *et al.* (2017) Mitochondrial O-GlcNAc transferase (mOGT) regulates mitochondrial structure, function, and survival in HeLa cells. J. Biol. Chem., 292, 4499–4518.
19. Jackson, S.P. *et al.* (1988) O-glycosylation of eukaryotic transcription factors: implications for mechanisms of transcriptional regulation. Cell, 55, 125–133.
20. Golks, A. *et al.* (2007) Requirement for O-linked N-acetylglucosaminyltransferase in lymphocytes activation. EMBO J., 26, 4368–4379.
21. Dentin, R. *et al.* (2008) Hepatic glucose sensing via the CREB coactivator CRTC2. Science, 319, 1402–1405.
22. Housley, M.P. *et al.* (2008) O-GlcNAc regulates FoxO activation in response to glucose. J. Biol. Chem., 283, 16283–16292.
23. Ruan, H.B. *et al.* (2012) O-GlcNAc transferase/host cell factor C1 complex regulates gluconeogenesis by modulating PGC-1α stability. Cell Metab., 16, 226–237.
24. Han, I. *et al.* (1997) Reduced O glycosylation of Sp1 is associated with increased proteasome susceptibility. Mol. Cell. Biol., 17, 2550–2558.
25. Kelly, W.G. *et al.* (1993) RNA polymerase II is a glycoprotein. Modification of the COOH-terminal domain by O-GlcNAc. J. Biol. Chem., 268, 10416–10424.
26. Wu, D. *et al.* (2017) Potential coordination role between O-GlcNAcylation and epigenetics. Protein Cell, 8, 713–723.
27. Gambetta, M.C. *et al.* (2015) A critical perspective of the diverse roles of O-GlcNAc transferase in chromatin. Chromosoma, 124, 429–442.
28. Hirosawa, M. *et al.* (2016) Novel O-GlcNAcylation on Ser(40) of canonical H2A isoforms specific to viviparity. Sci. Rep., 6, 31785.
29. Lercher, L. *et al.* (2015) Generation of a synthetic GlcNAcylated nucleosome reveals regulation of stability by H2A-Thr101 GlcNAcylation. Nat. Commun., 6, 7978.
30. Chen, Q. *et al.* (2016) OGT restrains the expansion of DNA damage signaling. Nucleic Acids Res., 44, 9266–9278.
31. Rønningen, T. *et al.* (2015) Prepatterning of differentiation-driven nuclear lamin A/C-associated chromatin domains by GlcNAcylated histone H2B. Genome Res., 25, 1825–1835.
32. Hahne, H. *et al.* (2012) Discovery of O-GlcNAc-modified proteins in published large-scale proteome data. Mol. Cell. Proteomics, 11, 843–850.
33. Fujiki, R. *et al.* (2011) GlcNAcylation of histone H2B facilitates its monoubiquitination. Nature, 480, 557–560.
34. Sakabe, K. *et al.* (2010) Beta-N-acetylglucosamine (O-GlcNAc) is part of the histone code. Proc. Natl. Acad. Sci. USA, 107, 19915–19920.
35. Schouppe, D. *et al.* (2011) Interaction of the tobacco lectin with histone proteins. Plant Physiol., 155, 1091–1102.
36. Hanover, J.A. *et al.* (2012) Bittersweet memories: linking metabolism to epigenetics through O-GlcNAcylation. Nat. Rev. Mol. Cell Biol., 13, 312–321.
37. Lewis, B.A. *et al.* (2014) O-GlcNAc and the epigenetic regulation of gene expression. J. Biol. Chem., 289, 34440–34448.
38. Chen, Q. *et al.* (2013) TET2 promotes histone O-GlcNAcylation during gene transcription. Nature, 493, 561–564.
39. Deplus, R. *et al.* (2013) TET2 and TET3 regulate GlcNAcylation and H3K4 methylation through OGT and SET1/COMPASS. EMBO J., 32, 645–655.
40. Daou, S. *et al.* (2011) Crosstalk between O-GlcNAcylation and proteolytic cleavage regulates the host cell factor-1 maturation pathway. Proc. Natl. Acad. Sci. USA, 108, 2747–2752.
41. Capotosti, F. *et al.* (2011) O-GlcNAc transferase catalyzes site-specific proteolysis of HCF-1. Cell, 144, 376–388.
42. Wysocka, J. *et al.* (2003) Human Sin3 deacetylase and trithorax-related Set1/Ash2 histone H3-K4 methyltransferase are tethered together selectively by the cell-proliferation factor HCF-1. Genes Dev., 17, 896–911.
43. Gambetta, M.C. *et al.* (2009) Essential role of the glycosyltransferase sxc/Ogt in polycomb repression. Science, 325, 93–96.
44. Myers, S.A. *et al.* (2011) Polycomb repressive complex 2 is necessary for the normal site-specific O-GlcNAc distribution in mouse embryonic stem cells. Proc. Natl. Acad. Sci. USA, 108, 9490–9495.
45. Dehennaut, V. *et al.* (2014) O-GlcNAcylation, an epigenetic mark. Focus on the histone code, TET family proteins, and polycomb group proteins. Front. Endocrinol. (Lausanne), 5, 155.
46. Zhang, Y. *et al.* (1999) Analysis of the NuRD subunits reveals a histone deacetylase core complex and a connection with DNA methylation. Genes Dev., 13, 1924–1935.
47. Lai, A.Y. *et al.* (2011) Cancer biology and NuRD: a multifaceted chromatin remodelling complex. Nat. Rev. Cancer, 11, 588–596.
48. Denslow, S.A. *et al.* (2007) The human Mi-2/NuRD complex and gene regulation. Oncogene, 26, 5433–5438.
49. Wang, Y. *et al.* (2009) LSD1 is a subunit of the NuRD complex and targets the metastasis programs in breast cancer. Cell, 138, 660–672.
50. Si, W. *et al.* (2015) Dysfunction of the reciprocal feedback loop between GATA3- and ZEB2-nucleated repression programs contributes to breast cancer metastasis. Cancer Cell, 27, 822–836.
51. Cano, A. *et al.* (2000) The transcription factor snail controls epithelial-mesenchymal transitions by repressing E-cadherin expression. Nat. Cell Biol., 2, 76–83.
52. Batlle, E. *et al.* (2000) The transcription factor snail is a repressor of E-cadherin gene expression in epithelial tumour cells. Nat. Cell Biol., 2, 84–89.
53. Garkavtsev, I. *et al.* (2004) The candidate tumour suppressor protein ING4 regulates brain tumour growth and angiogenesis. Nature, 428, 328–332.
54. Shiseki, M. *et al.* (2003) p29ING4 and p28ING5 bind to p53 and p300, and enhance p53 activity. Cancer Res., 63, 2373–2378.
55. Lánczky, A. *et al.* (2016) miRpower: a web-tool to validate survival-associated miRNAs utilizing expression data from 2178 breast cancer patients. Breast Cancer Res. Treat., 160, 439–446.
56. Cheung, W.D. *et al.* (2008) O-linked beta-N-acetylglucosaminyltransferase substrate specificity is regulated by myosin phosphatase targeting and other interacting proteins. J. Biol. Chem., 283, 33935–33941.
57. Toleman, C. *et al.* (2004) Characterization of the histone acetyltransferase (HAT) domain of a bifunctional protein with activable O-GlcNAcase and HAT activities. J. Biol. Chem., 279, 53665–53673.
58. Whisenhunt, T.R. *et al.* (2006) Disrupting the enzyme complex regulating O-GlcNAcylation blocks signaling and development. Glycobiology, 16, 551–563.
59. Zhang, Q. *et al.* (2014) Differential regulation of the ten-eleven translocation (TET) family of dioxygenases by O-linked β-N-acetylglucosamine transferase (OGT). J. Biol. Chem., 289, 5986–5996.
60. Vella, P. *et al.* (2013) Tet proteins connect the O-linked N-acetylglucosamine transferase Ogt to chromatin in embryonic stem cells. Mol. Cell, 49, 645–656.
61. Shi, F.T. *et al.* (2013) Ten-eleven translocation 1 (Tet1) is regulated by O-linked N-acetylglucosamine transferase (Ogt) for target gene repression in mouse embryonic stem cells. J. Biol. Chem., 288, 20776–20784.
62. Chu, C.S. *et al.* (2014) O-GlcNAcylation regulates EZH2 protein stability and function. Proc. Natl. Acad. Sci. USA, 111, 1355–1360.

63. Xue, Y. *et al.* (1998) NURD, a novel complex with both ATP-dependent chromatin-remodeling and histone deacetylase activities. Mol. Cell, 2, 851–861.
64. Nieto, M.A. (2002) The snail superfamily of zinc-finger transcription factors. Nat. Rev. Mol. Cell Biol., 3, 155–166.
65. Fujita, N. *et al.* (2003) MTA3, a Mi-2/NuRD complex subunit, regulates an invasive growth pathway in breast cancer. Cell, 113, 207–219.
66. Feng, X. *et al.* (2002) Different HATS of the ING1 gene family. Trends Cell Biol., 12, 532–538.
67. He, G.H. *et al.* (2005) Phylogenetic analysis of the ING family of PHD finger proteins. Mol. Biol. Evol., 22, 104–116.
68. Unoki, M. *et al.* (2009) Reviewing the current classification of inhibitor of growth family proteins. Cancer Sci., 100, 1173–1179.
69. Coles, A.H. *et al.* (2009) The ING gene family in the regulation of cell growth and tumorigenesis. *J Cell Physiol*, 218, 45–57.
70. Kim, S. *et al.* (2010) A dominant mutant allele of the ING4 tumor suppressor found in human cancer cells exacerbates MYC-initiated mouse mammary tumorigenesis. Cancer Res., 70, 5155–5162.
71. Yan, R. *et al.* (2015) SCF(JFK) is a bona fide E3 ligase for ING4 and a potent promoter of the angiogenesis and metastasis of breast cancer. Genes Dev., 29, 672–685.
72. Goldberg, A.D. *et al.* (2007) Epigenetics: a landscape takes shape. Cell, 128, 635–638.
73. Sharma, S. *et al.* (2010) Epigenetics in cancer. Carcinogenesis, 31, 27–36.
74. Herceg, Z. (2007) Epigenetics and cancer: towards an evaluation of the impact of environmental and dietary factors. Mutagenesis, 22, 91–103.
75. Hardy, T.M. *et al.* (2011) Epigenetic diet: impact on the epigenome and cancer. Epigenomics, 3, 503–518.
76. Lim, U. *et al.* (2012) Dietary and lifestyle factors of DNA methylation. Methods Mol. Biol., 863, 359–376.
77. Jiménez-Chillarón, J.C. *et al.* (2012) The role of nutrition on epigenetic modifications and their implications on health. Biochimie, 94, 2242–2263.
78. Zeng, Q. *et al.* (2016) O-linked GlcNAcylation elevated by HPV E6 mediates viral oncogenesis. Proc. Natl. Acad. Sci. USA, 113, 9333–9338.